A Cascaded Boost-Buck Converter for High Efficiency Wireless Power Transfer Systems

Minfan Fu, *Student Member, IEEE,* Chengbin Ma, *Member, IEEE,* Xinen Zhu, *Member, IEEE*

Abstract—Wireless power transfer (WPT) has attracted an ever increasing interest from both industry and academics over the past few years. Its applications vary from small power devices such as mobile phones and tablets to high power electric vehicles, and from small transfer distance of centimeters to large distance of tens of centimeters. In order to achieve a high efficiency WPT system, each circuit should function at a high efficiency along with proper impedance matching techniques to minimize the power reflection due to impedance mismatch. This paper proposes an analysis on the system efficiency to determine the optimal impedance requirement for coils, rectifier and DC-DC converter. A novel cascaded boost-buck DC-DC converter is designed to provide the optimal impedance matching in WPT system for various loads including resistive load, ultracapacitors and batteries. The proposed 13.56 MHz WPT system can achieve a total system efficiency over 70% in experiment.

Index Terms—wireless power transfer, inductive resonance coupling, power reflection, DC-DC converter

I. INTRODUCTION

Maxwell's equations mathematically predict that electromagnetic waves, as a carrier of energy, can propagate in space, which leads to the revolutionary development of wireless communication, thus change the modern society in numerous ways. Based on the same physics, a much larger amount of energy, compared to that of digital bits in wireless communication, can be transferred wirelessly over a long distance. This idea of wireless power transfer was first proposed by Nikola Tesla in 1904 as a "world system" for "the transmission of electrical energy without wires" that applied capacitive coupling [1]. In recent years there is a renewed interest in the research and applications of wireless power transfer due to a dramatic need to wirelessly charge many consumer electronic devices (smart phones, laptop computers, tablets, computer peripherals). It is desired by end users to cut the last cord (electrical charging wire) so that a ubiquitous access to both information and electrical power through air is for the first time feasible. For more power hungry devices and systems, such as robots and electric vehicles, wireless charging not only provides an easier and safer experience of high voltage and high current daily charging process, but also enables a totally new direction of management of electrical power

M. Fu, C. Ma and X. Zhu are with University of Michigan-Shanghai Jiaotong University Joint Institute, Shanghai Jiao Tong University, 800 Dongchuan Road, Minhang, Shanghai 200240, P.R. China (e-mail: zhuxinen@sjtu.edu.cn).

efficiently. For example, batteries are widely recognized as a clean technology for hybrid and pure electric vehicles though the specific energy of petrol ($\sim$12,432Wh/kg) is hundreds of times that of a mass-market battery (20-200Wh/kg) [2], [3]. However for electric vehicles to replace conventional engine cars driven by fossil based energy totally, there are several challenges for batteries to be addressed, such as limited energy density, slow charging speed, reliability, weight, cost, and etc. One of the major concerns of electric vehicles today is the limited cruise range with a full charge, which ranges from 100 to 150 km. The wireless charging, on the other hand, provides an alternative solution without requiring dramatic improvements in battery technology [4], [5].

Various wireless power transfer technologies exist for different applications, such as inductive coupling, magnetic resonance coupling, microwave and laser radiation. Depending on the power level of interest, transfer distance, size and form factors, each technology may be more suitable for certain scenario than the others. Microwave and laser radiation use far field to transfer electric power wirelessly, therefore the transfer distance can be over meters, even hundreds of meters, but with a relative small output power due to the potential hazardous radiation to human being and other electronic devices [6], [7]. Besides, for a focused radiation beam, a large size antenna array is usually required. On the contrary, the inductive coupling and magnetic resonance coupling use near field to transfer power. Though the transfer distance is usually limited to several centimeters, the output power can be as high as tens of kilowatts. The magnetic resonance coupling occurs when power sources and receiving devices are specially designed magnetic resonators with approximately same natural frequencies, i.e. resonant inductive coupling using the inherent capacitances of the coils [8]. The inductive coupling systems are also usually tuned to resonance but using external capacitances [9], [10]. As another near-field method, inductive coupling is a mature technique that is widely used today for both low and high power applications [11]–[13]. The inductive coupling systems usually operate in kHz band such as at 20 kHz mostly because the state-of-art power electronic devices are available for both power generation and conditioning. On the other hand, higher frequency is generally desired for more compact and lighter resonators. However, there are restrictions on the usable frequency range under the regulation of ISM (industrial, scientific and medical) band and the performances of power switching devices [14], [15].

For all the above mentioned wireless power transfer technologies, they share a same system architecture which consists of a power source to generate electrical power, a coupling

system (coils or antennas) to transmit and receive power wirelessly, a rectifying circuit to convert the AC power to DC power, and a power regulating and charging management circuit (usually a DC-DC converter). As an example, Fig. 1 illustrates a wireless power transfer system using resonant inductive coupling operating at 13.56 MHz. For such a system to transfer power efficiently, each circuit should be designed for its highest efficiency, and the power reflection between any two adjacent circuits should be minimized. High efficient power sources are usually realized in highly nonlinear switching power amplifiers, such as class D or class E topologies. Coils with high quality factors are desired for low power loss, and magnetic materials are used to shape the magnetic field for tight coupling in order to increase the transfer efficiency too. It is a common practice to insert an impedance matching network between circuits to minimize the power reflection due to impedance mismatch. Though this is a straightforward method to overcome power reflection, the impedance matching network itself may introduce additional power loss due to unavoidable non ideal capacitors and inductors, as well as extra space and weight to the system. Furthermore a battery or ultracapacitor presents a changing impedance to the whole system during the charging process, which means a fixed design of impedance matching network may not function at its designed performance as the load is changing over time. In this paper, a new method is proposed to increase the overall efficiency of wireless power transfer system without impedance matching networks. Other than the conventional way in which each circuit is designed separately then combined together, we analyze the whole system for high efficiency and derive the impedance requirement for each circuit. A novel buck-boost DC-DC converter is proposed to provide an optimal impedance for minimal power reflection. At the same time this DC-DC converter minimizes the effect of a dynamic load to the system efficiency, therefore alleviates the need of a tunable impedance matching network. The method of this paper can be applied to any general WPT system without restrictions on the selection of power sources, coupling coils and rectifying circuits.

The paper is organized in the following way. In Section II a detailed equivalent circuit model for the coupling system is described using the concept of scattering matrix that is widely used in designing microwave circuits. Then the requirement on an optimal impedance is analyzed in order to achieve a maximum power transfer efficiency. In Section III a cascaded boost-buck converter is proposed to perform the impedance matching, by which any resistive or capacitive load can be matched to a specified impedance. Then in Section IV the analysis and circuit design for the impedance matching are validated by experimental results. Finally the conclusion is drawn in Section V.

II. ANALYSIS ON SYSTEM EFFICIENCY

A. Equivalent Circuit Model of Resonant Coils

Fig. 2 shows the general configuration of a wireless power transfer system using resonant inductive coupling. The system consists of an AC source with an equivalent internal impedance Z_S, two resonance coils and a load impedance Z_L. Two
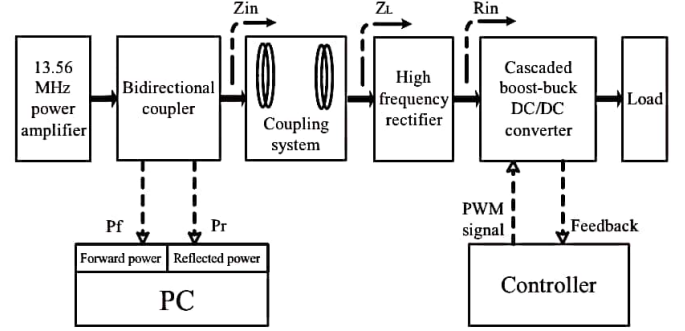

Fig. 1. The configuration of the 13.56MHz wireless power transfer system

identical open-circuit coils are used in the final system because of their simple electrical circuit model for theoretical analysis and simple structure for fabrication in the lab. The two coils are tuned to resonant using external capacitors or the parasitic capacitances of the coils. The equivalent circuit model of the system is shown in Fig. 3(a). In the model, both the transmitting and receiving coil are represented as a series RLC circuit, and the magnetic coupling is described by the mutual inductance L_m [16], [17].
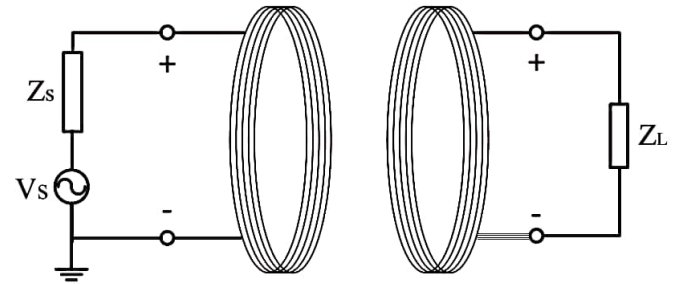

Fig. 2. A simplified system configuration of a wireless power transfer system.

In this paper, scattering matrix ([S] matrix) is introduced to analyze the power reflection and transmission characteristics of the coils, from which an optimal load impedance at the receiving coil can be designed to minimize the power loss due to impedance mismatching. The [S] matrix for the two-port equivalent circuit model is defined as

$$\begin{bmatrix} V_1^- \\ V_2^- \end{bmatrix} = \begin{bmatrix} S_{11} & S_{12} \\ S_{21} & S_{22} \end{bmatrix} \begin{bmatrix} V_1^+ \\ V_2^+ \end{bmatrix}, \qquad (1)$$

where V_i^+ is the voltage wave incident on port i, and V_i^- is the voltage wave reflected from port i ($i = 1, 2$). Based on the equivalent circuit model, the scattering parameters for the two resonant coils are derived as

$$S_{11} = S_{22} =$$
$$\frac{(-Z_0 + R + j\omega L + \frac{1}{j\omega C})(Z_0 + R + j\omega L + \frac{1}{j\omega C}) + \omega^2 L_m^2}{(Z_0 + R + j\omega L + \frac{1}{j\omega C})^2 + \omega^2 L_m^2}$$
$$\qquad (2)$$

$$S_{21} = S_{12} = \frac{2j\omega L_m Z_0}{(Z_0 + R + j\omega L + \frac{1}{j\omega C})^2 + \omega^2 L_m^2} \qquad (3)$$
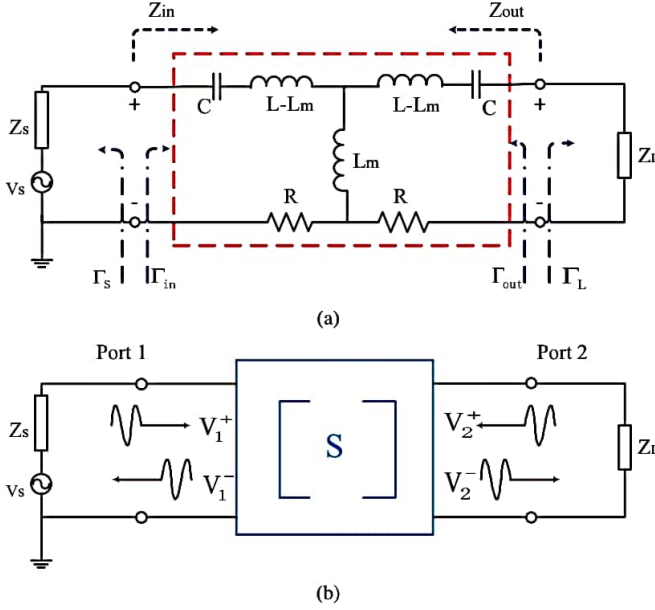
Fig. 3. Equivalent circuit model of WPT system and its representation using [S] matrix. (a) Equivalent circuit model. (b) The two port model described by [S] matrix.

where Z_0 is the system characteristic impedance, which is usually 50 Ω [18].

The corresponding reflection coefficients for the source and the load, Γ_S and Γ_L are given as

$$\Gamma_s = \frac{Z_s - Z_0}{Z_s + Z_0} \tag{4}$$

and

$$\Gamma_L = \frac{Z_L - Z_0}{Z_L + Z_0}, \tag{5}$$

respectively. Combined with Eqs. (1)-(5), the reflection coefficients for the input port (i.e. port 1) and the output port (i.e. port 2) can be calculated as

$$\Gamma_{in} = \frac{V_1^-}{V_1^+} = S_{11} + \frac{S_{12}S_{21}\Gamma_L}{1 - S_{22}\Gamma_L} = \frac{Z_{in} - Z_0}{Z_{in} + Z_0} \tag{6}$$

and

$$\Gamma_{out} = \frac{V_2^-}{V_2^+} = S_{22} + \frac{S_{12}S_{21}\Gamma_s}{1 - S_{11}\Gamma_s} = \frac{Z_{out} - Z_0}{Z_{out} + Z_0}, \tag{7}$$

respectively. Z_{in} is the equivalent input impedance looking into the transmitting coil, and Z_{out} the equivalent input impedance looking into the receiving coil, as shown in Fig. 3(a).

The maximum power transfer from the source to the resonance coils can be achieved when conjugate matching occurs, namely $\Gamma_{in} = \Gamma_s^*$. Similarly, the condition of $\Gamma_{out} = \Gamma_L^*$ enables the maximum power transfer from the resonance coils to the load. Under the resonance condition by

$$j\omega L + \frac{1}{j\omega C} = 0, \tag{8}$$

and from Eqs. (2)(3)(6)(7), the simultaneous conjugate matchings at both the input and output ports, $\Gamma_{in} = \Gamma_s^*$ and

$\Gamma_{out} = \Gamma_L^*$ give

$$\Gamma_S = \Gamma_L = S_{11} \pm \mid S_{12} \mid = \frac{(-Z_0 + R)(Z_0 + R) + \omega^2 L_m^2 \pm 2\omega L_m Z_0}{(Z_0 + R)^2 + \omega^2 L_m^2}. \tag{9}$$

Combined with Eqs. (4)(5), the optimal source and load impedances, Z_S and Z_L can be solved as

$$Z_{S,opt} = Z_{L,opt} = \frac{w^2 L_m^2 + R^2 + RZ_0 \pm wL_m Z_0}{Z_0 + R \mp wL_m}. \tag{10}$$

Therefore, for a specific pair of resonant coils with fixed R, L, C and L_m, the optimal source and load impedances are then determined by (10) in order to achieve maximum power transfer.

However, the above derived optimal source and load impedance may not be easily satisfied in real applications where the source impedance Z_s is usually designed to match a standard impedance such as 50 Ω for radio frequency (RF) power sources. Thus, the maximum power transfer for a WPT system with a predefined Z_s can be achieved through an optimal load impedance Z_L. As shown in Fig. 3(a), the input impedance seen by the source is derived as

$$Z_{in} = \frac{(R + j\omega L + \frac{1}{j\omega C})(Z_L + R + j\omega L + \frac{1}{j\omega C}) + \omega^2 L_m^2}{Z_L + R + j\omega L + \frac{1}{j\omega C}}, \tag{11}$$

which equals to

$$R + \frac{\omega^2 L_m^2}{Z_L + R} \tag{12}$$

under the resonance [refer to Equ. (8)]. Accordingly, the optimal load impedance that enables $Z_{in} = Z_S^*$ can be calculated as

$$Z'_{L,opt} = \frac{\omega^2 L_m^2}{Z_S^* - R} - R. \tag{13}$$

Tbl. I lists the parameters of the resonance coils in the following experimental WPT system described in sec. IV. These electrical parameters can be obtained by fitting the equivalent circuit model to the S-parameters measured by the Vector Network Analyzer. The coils are the two identical open-circuit helical coils without external capacitors. The power source is a 13.56 MHz power amplifier (PA) whose source impedance is 50 Ω. Here the system efficiency η is defined as

$$\eta = \frac{P_l}{P_f}, \tag{14}$$

where P_f is the forward power from PA and P_l is the power received by Z_L, respectively [refer to Fig. 2]. As shown in Fig. 4, two cases are simulated. The black curve is for the case with variable source impedance, namely $Z_s = Z_L = Z$, while the red one for the case with fixed source impedance $Z_s = 50$ Ω and $Z_L = Z$. The case of variable source impedance (i.e. the black curve) show limited improvement in maximum system efficiency over the case of fixed 50 Ω source impedance (i.e. the red curve). Considering design complexity, it is practical to control only the load impedance. The optimal load impedance $Z'_{L,opt}$ is found to be 73 Ω by the simulation, which matches the calculation result using Equ. (13) and the coil parameters in Tbl. I. At this optimal load impedance the transfer efficiency of the coupling coils is found to be about 90%.

TABLE I
PARAMETERS OF THE TWO RESONANCE COILS

Coil diameter	320 mm
Coils gap	150 mm
Resonant frequency	13.56 MHz
Inductance L	7.8 μH
Capacitance C	17.6 pF
Internal resistance R	3.4 Ω
Mutual Inductance L_m	0.7 μH
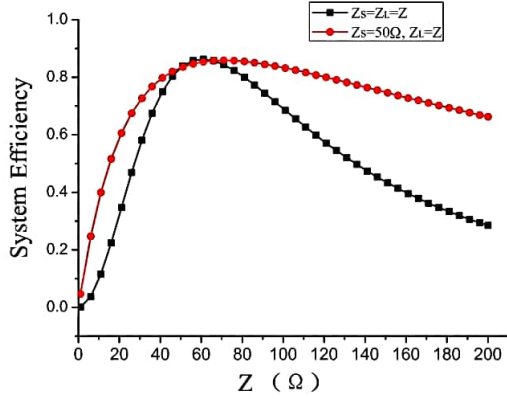
Fig. 4. System efficiency with variable source impedance (black) and fixed source impedance (red).

(a)

(b)

Fig. 5. System efficiency analysis with rectifier. (a) System configuration in ADS. (b) System efficiency versus load resistance.

B. Optimal Load Resistance to Rectifier

In the previous subsection, an optimal load impedance to the receiving coil has been derived for maximum power transfer. This impedance is realized as the equivalent input impedance of the following circuits, which usually include a rectifier, a DC-DC converter and the actual load to be charged electrically. For a conventional full bridge rectifier, such as shown in Fig. 5(a), there exists a corresponding optimal load resistance R_L to generate the required optimal impedance Z_L. This R_L also depends on the operating frequency, the characteristics of Schottky diodes, input power level in the rectifier. The exact analytical expression of R_L is difficult to obtain due to the nonlinear nature of rectifiers and complex model of Schottky diodes. Instead nonlinear circuit simulation tool is used, which is the Advanced Design System (ADS) from Agilent. In the ADS simulation, the resonance coils are simulated using it s-parameter data (S2P file) measured by network analyzer, and the SiC Schottky diodes (STPSC406) using their Pspice model.

Here the system efficiency refers to the ratio of the power P_l received by R_L and the forward power P_f from PA. As shown in Fig. 5(b) and Fig. 6, there is an optimal R_L, 98 Ω for a maximum efficiency of 81 %, while Z_L deviates from its optimal value. i.e. 73 Ω. In addition, the optimal $Z'_{L,opt}$ can not be achieved by adjusting the value of R_L, namely the existence of impedance mismatch [see Fig. 6]. If a matching network is added between the resonance coils and the rectifier, the system efficiency can be improved from 81% to 83% with $R_L = 98$ Ω and ideal L and C models, while the efficiency drops to 82% if realistic L and C models are used. Considering the limited efficiency improvement and increased system complexity, only
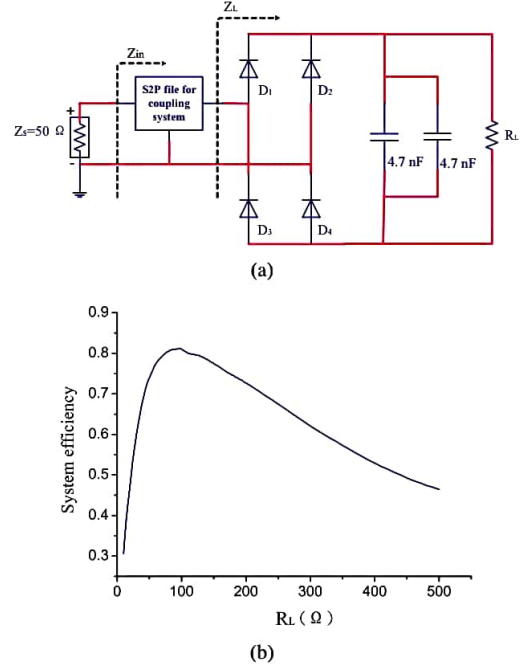
the impedance matching after the rectifier is proposed in this paper, which is realized by using a novel boost-buck DC-DC converter [refer to Fig. 1].
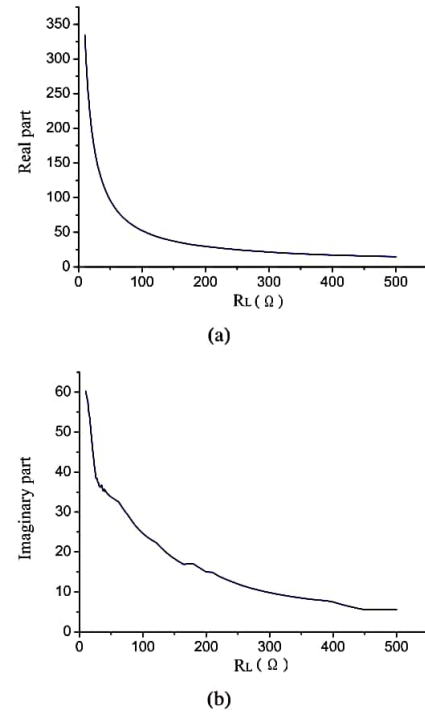

(a)

(b)

Fig. 6. Impedance Z_L seen by the resonance coils when sweeping R_L. (a) Real part. (b) Imaginary part.

III. DC-DC CONVERTER

A. Review of Basic Topologies

DC-DC converters can be utilized to control equivalent load resistance. The six basic DC-DC converter topologies, buck, boost, buck-boost, Ćuk, Single-Ended Primary-Inductor Converter (SEPIC) and Zeta converters are shown in Fig. 7. For the buck converter, assume there is no power loss, then

$$\frac{V_{in}^2}{R_{in}} = \frac{V_{out}^2}{R_L}, \tag{15}$$

where V_{in} and V_{out} are the input and output voltages, respectively. R_{in} is input resistance (i.e. the load resistance seen by the rectifier), and here R_L is the load resistance for the DC-DC converter. Since

$$V_{out} = DV_{in}, \tag{16}$$

where D is the duty cycle, then

$$R_{in} = \frac{R_L}{D^2} \tag{17}$$

The equivalent input resistance for other five topologies can be similarly derived. The characteristics of the six DC-DC converter topologies in terms of equivalent input resistance adjustment are summarized in Tbl. II, where I_{in} is input current.
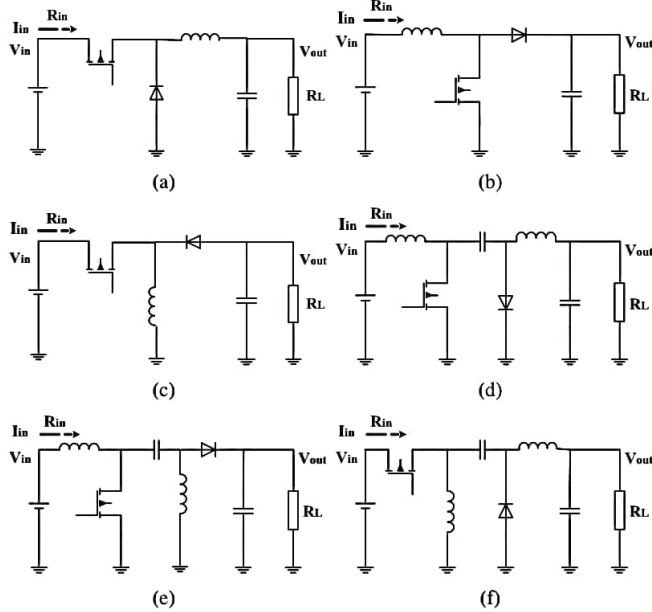

Fig. 7.   Basic DC-DC converter topologies. (a) Buck. (b) Boost. (c) Buck-boost. (d) Ćuk. (e) SEPIC. (f) Zeta.

Meanwhile, constant duty cycle control is incapable to deal with a variable load. It is straightforward to directly control the ratio of input voltage V_{in} to input current I_{in} in order to achieve a constant input resistance R_{in}. From the viewpoint of implementation, the boost, Ćuk and SEPIC topologies are more suitable because their continuous input current is easier to control.

Topology	V_{out}	R_{in}	R_{in} (range)	I_{in}
Buck	DV_{in}	$\frac{R_L}{D^2}$	$R_L \sim +\infty$	Discontinuous
Boost	$\frac{1}{1-D}V_{in}$	$(1-D)^2 R_L$	$0 \sim R_L$	Continuous
Buck-boost	$\frac{D}{1-D}V_{in}$	$\frac{(1-D)^2}{D^2}R_L$	$0 \sim +\infty$	Discontinuous
Ćuk	$\frac{-D}{1-D}V_{in}$	$\frac{(1-D)^2}{D^2}R_L$	$0 \sim +\infty$	Continuous
SEPIC	$\frac{D}{1-D}V_{in}$	$\frac{(1-D)^2}{D^2}R_L$	$0 \sim +\infty$	Continuous
Zeta	$\frac{D}{1-D}V_{in}$	$\frac{(1-D)^2}{D^2}R_L$	$0 \sim +\infty$	Discontinuous

B. Cascaded Boost-Buck Converter

As shown in Tbl. II, the boost converter has a limited range of input resistance adjustment, while it is known that the Ćuk converter has opposite polarity between input and output. As shown in Fig. 8, considering the needs of battery charging and power management, a cascaded boost-buck DC-DC converter topology is proposed, which can be controlled to match any given load. The input resistance of boost converter is easy to control due to its continuous input current feedback, while the buck converter is widely used in battery charging and power management. It is convenient to control and predict the behavior of the cascaded converter because the boost and buck converters can be separately analyzed. Compared with the traditional "one-switch" topologies, the boost-buck "two-switch" topology provides more flexibility in the design and control of wireless power transfer systems. There are two control modes of the cascaded boost-buck converter, fixed load mode and variable load mode, respectively.
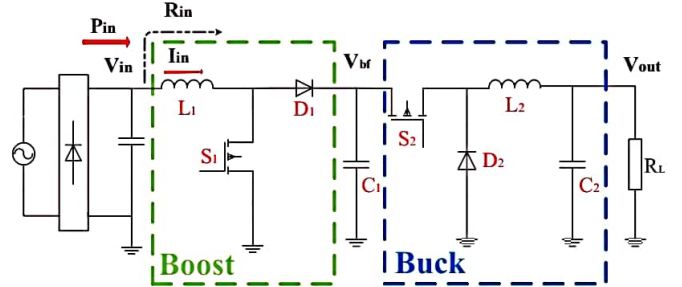

Fig. 8.   Cascaded boost-buck converter topology

1) Fixed load mode: Constant duty cycle control is applied. The input resistance of the cascaded boost-buck DC-DC converter can be derived as follows. Since

$$V_{bf} = \frac{1}{1-D_1}V_{in} \tag{18}$$

and

$$V_{out} = D_2 V_{bf}, \tag{19}$$

Assuming there is no power loss, then

$$\frac{V_{in}^2}{R_{in}} = \frac{V_{out}^2}{R_L} \tag{20}$$

gives

$$R_{in} = \left(\frac{1-D_1}{D_2}\right)^2 R_L, \tag{21}$$

where V_{bf} is buffer capacitor voltage. D_1 and D_2 are the duty cycles of the switches S_1 and S_2, respectively. For the sake of simplicity, letting D_1 equal D_2 gives the duty cycle D that needs to be controlled as

$$D = \frac{1}{\sqrt{\frac{R_{in}}{R_L} + 1}}. \tag{22}$$

Theoretically any resistive load can be matched to any specific value using the constant duty cycle control.

2) Variable load mode: For a general wireless power transfer system, its load may have significantly varying characteristics. Constant duty cycle control is not valid in such case. For the dynamic control of the equivalent input resistance R_{in}, three feedback signals need to be measured, which are input voltage V_{in}, input current I_{in} and buffer capacitor voltage V_{bf}. The duty cycle D_1 is controlled to maintain a fixed ratio of V_{in} to I_{in}, while D_2 is controlled to provide a V_{bf} that is higher than V_{in} such as $V_{bf} = kV_{in}$ with $k > 1$. Since

$$R_{in} = \frac{V_{in}}{I_{in}} = \frac{V_{in}^2}{P_{in}} \tag{23}$$

and

$$V_{bf} = \frac{1}{1 - D_1}V_{in}, \tag{24}$$

then R_{in} can be represented as

$$R_{in} = \frac{V_{bf}^2(1 - D_1)^2}{P_{in}}, \tag{25}$$

where P_{in} is the input power that equals $V_{in} \cdot I_{in}$.

The control blockdiagram for the variable load mode is shown in Fig. 9. Input current I_{in}, input voltage V_{in} and buffer capacitor voltage V_{bf} are the three feedback signals for the control of D_1 and D_2, namely the duty cycles for the boost and buck converters, respectively [refer to Fig. 8]. There are two PI controllers for the control of the equivalent load resistance and the buffer capacitor voltage, respectively. The upper PI controller minimizes control error $R_{in}^* I_{in} - V_{in}$, where R_{in}^* is the optimal load resistance seen by the rectifier. The lower PI controller regulates V_{bf} to be equal with kV_{in}, where k is greater than one.
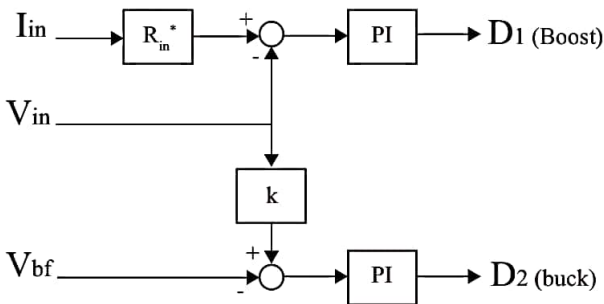

Fig. 9. Duty cycle control blockdiagram for the variable load mode.

C. Implementation

The circuit board of the cascaded boost-buck converter is shown in Fig. 10(a), which is designed and fabricated in house. The switching frequency of the DC-DC converter is 20 kHz and its dimension is 220 mm×160 mm. The efficiency is verified in the fixed load mode. The overall efficiency of the DC-DC converter is about 90%. The low efficiency at low power range is mainly caused by the switching loss.
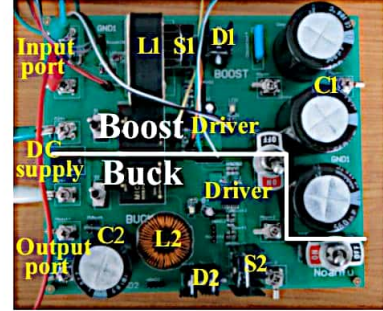
(a)
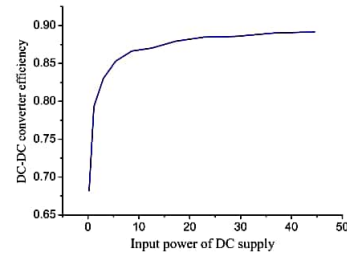
(b)

Fig. 10. Cascaded boost-buck converter. (a) Circuit board. (b) Efficiency.

IV. EXPERIMENTAL VERIFICATION

The testing wireless power transfer system is shown in Fig. 11, which consists of a 13.56 MHz class-D PA, a bidirectional coupler for the sensing of forward and reflected power (P_f and P_r), two resonance coils, a rectifier using SiC Schottky diodes, a boost-buck DC-DC converter for impedance matching and various loads. The matching for three types of load are verified including resistive load, Lithium-ion battery and ultracapacitor. The resistive load is emulated by using electric load. The specifications for the battery bank and ultracapacitor bank are listed in Tbl. III and Tbl. IV, respectively. In experiments, the duty cycle control is implemented using TI DSP 28335. P_f and P_r can be directly measured by the bidirectional coupler and two power sensors. The load power P_l is determined by the measurement of voltage and current on the load. A general purpose class-D power amplifier is used as the PA with an efficiency of about 80%. 40 Watts forward power from the power amplifier is chosen to demonstrate a medium power transfer capability. The system efficiency here is the ratio of the power received by the above three types of the load, P_l and the forward power P_f from the PA.
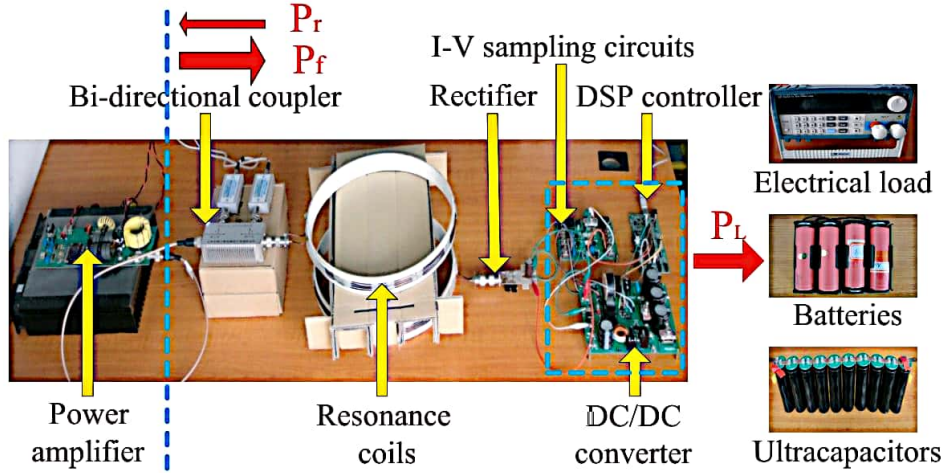
Fig. 11.   The testing wireless power transfer system with various loads

TABLE III
LITHIUM-ION BATTERY BANK

Capacity of single battery cell [Ah]	2.5
Voltage range of single battery [V]	3.7-4.2
Number of battery cells	4
Connection of cells	Serial

TABLE IV
ULTRACAPACITOR BANK

Single cell capacitance [F]	700
Single cell maximum voltage [V]	2.7
Number of cells	10
Connection of cells	Serial

A. Fixed Load Mode

In the fixed load mode experiment, the WPT system delivers power to various resistive loads by an electric load. For each resistive load, the duty ratio of the DC-DC converter is swept and the corresponding system efficiency is recorded and plotted in Fig. 12. It is clearly that there exists an optimal value of the duty ratio D for each resistive load to achieve the highest system efficiency. This is because the DC-DC converter presents a desired load resistance to the rectifier by adjusting its duty ratio such that the power reflection within the system is minimized, as shown in Fig. 12(b). This efficiency improvement using a controlled DC-DC converter can be further verified in Fig. 13. Without impedance matching, the wireless power transfer system can only work efficiently in a limited range of load resistance. By having the cascaded boost-buck DC-DC converter for the optimal impedance matching, the system efficiency is significantly improved over a wide range of load resistance. Because the load resistance between 50 Ω and 150 Ω approximately is close to the optimal load resistance, the lower efficiency within the above range of load resistance using the DC-DC converter is caused by the loss of the DC-DC converter [see Fig. 13(a)].

B. Variable Load Mode

In practice the load to be charged may not be pure resistors, but ultracapacitors and/or batteries whose electrical impedance changes over time during the charging period. This kind of dynamic loading to the WPT system can cause a degradation of the system efficiency if no proper circuit is implemented. The proposed cascaded boost-buck DC-DC converter can automatically adjust its duty ratio for optimal system efficiency when charging a ultracapacitor and battery. In Fig. 14 and Fig. 15, both the ultracapacitor and battery's charging status over time is plotted with and without the proposed DC-DC converter. The experimental results shown that the proposed DC-DC converter can improve the system efficiency from 64% to 74% for charging a battery, and from 23% to 73% for charging a ultracapacitor.

V. CONCLUSION

In this paper a system level analysis on optimal impedance matching and a novel cascaded boost-buck DC-DC converter are proposed to achieve a high efficiency wireless power transfer system. This method is universal and applicable for all wireless power transfer technologies. The cascaded boost-buck DC-DC converter functions in two folds: one for optimal impedance matching for rectifier, coils and PA, the other for isolation of the dynamic load from the system. A 13.56 MHz wireless power transfer system is demonstrated experimentally to prove this method. At a power level of 40 Watts, the system efficiency from the source to the final load is measured over 70% for various loads including resistive loads, ultracapactiors and batteries. Future direction of this work is to introduce a feedback control mechanism to improve the system efficiency and to make the system more robust. The DC-DC converter needs to be improved with an additional function of specific charging algorithm for ultracapacitors and batteries. At the same time PA may be controlled to adjust its output power according to the real-time charging status of the load, through tuning the DC bias voltage to PA and input signal level. The authors are currently working on these further improvements and will report these data in the future publication.
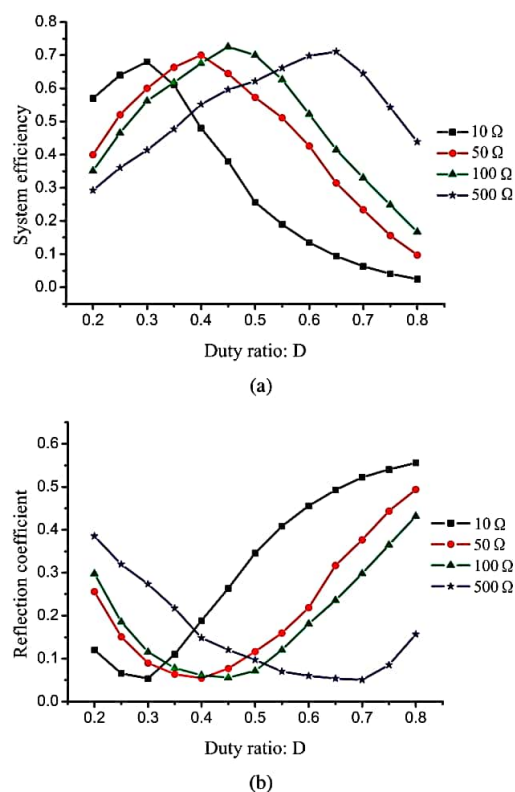
Fig. 12. System efficiency and reflection coefficient with various duty cycle *D*. (a) System efficiency. (b) Reflection coefficient.
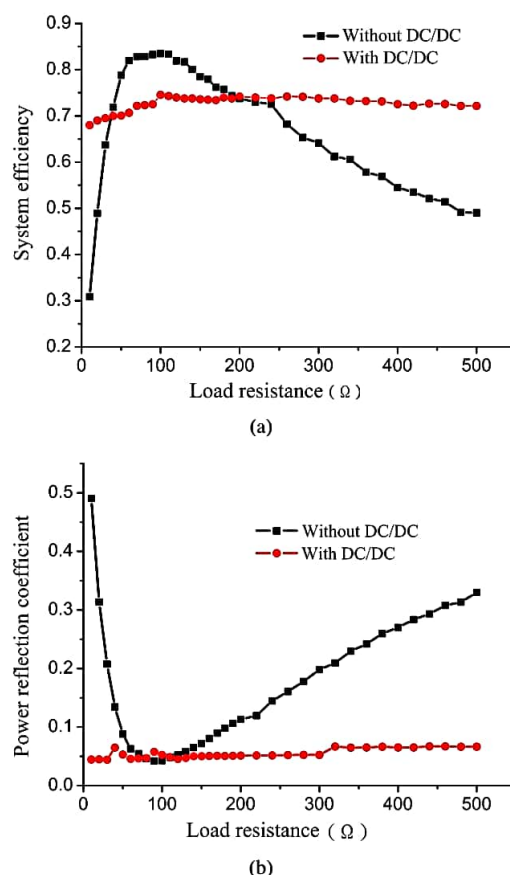

Fig. 13. System efficiency and reflection coefficient improvement using the cascaded boost-buck DC-DC converter. (a) System efficiency. (b) Reflection coefficient.
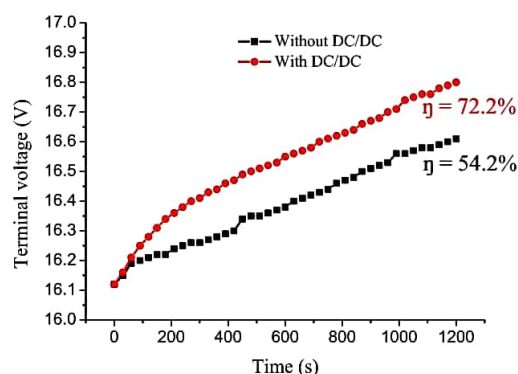

Fig. 14. Batteries charging improvement using the cascaded boost-buck DC-DC converter.

REFERENCES

[1] N. Tesla, "The transmission of electric energy without wires," *Electrical World and Engineer*, March 5, 1904.

[2] G. Thomas and C. San Ramon, "Overview of storage development doe hydrogen program," *Sandia National Laboratories*, vol. 9, 2000.

[3] F. Conte, "Battery and battery management for hybrid electric vehicles: a review," *E & i Elektrotechnik und Informationstechnik*, vol. 123, no. 10, pp. 424–431, 2006.

[4] J. Fishelson, K. Heaslip, W. Louisell, and K. Womack, "An evaluation framework for an automated electric transportation network," in *Proc. The 90th Transportation Research Board Annual Meeting*, Washington DC, Jan. 2011.

[5] H. Rakouth, J. Absmeier, A. Brown Jr, I.-S. Suh, R. Sumner, R. Henderson *et al.*, "EV charging through wireless power transfer: Analysis of efficiency optimization and technology trends," in *Proc. The FISITA 2012 World Automotive Congress*, Beijing, China, Nov. 2013, pp. 871–884.

[6] N. Shinohara, "Power without wires," *IEEE Microw. Mag.*, vol. 12, no. 7, pp. S64–S73, 2011.

[7] J. T. Howell, M. J. O'Neill, and R. L. Fork, "Advanced receiver/converter experiments for laser wireless power transmission," in *Proc. The 4th International Conference on Solar Power from Space (SPS04)*, vol. 567, Granada, Spain, 30 June–2 July 2004, pp. 187–194.

[8] A. Kurs, A. Karalis, R. Moffatt, J. D. Joannopoulos, P. Fisher, and M. Soljačić, "Wireless power transfer via strongly coupled magnetic resonances," *Science*, vol. 317, no. 5834, pp. 83–86, 2007.

[9] C.-S. Wang, O. H. Stielau, and G. A. Covic, "Design considerations for a contactless electric vehicle battery charger," *IEEE Trans. Ind. Electron.*, vol. 52, no. 5, pp. 1308–1314, 2005.

[10] A. P. Hu, *Wireless/Contactless Power Supply:-Inductively coupled resonant converter solutions*. VDM Publishing, 2009.

[11] N. A. Keeling, G. A. Covic, and J. T. Boys, "A unity-power-factor ipt pickup for high-power applications," *IEEE Trans. Ind. Electron.*, vol. 57, no. 2, pp. 744–751, 2010.

[12] K. Kobayashi, T. Pontefract, Y. Kamiya, and Y. Daisho, "Development and performance evaluation of a non-contact rapid charging inductive power supply system for electric micro-bus," in *Proc. The 7th IEEE Vehicle Power and Propulsion Conference (VPPC'11)*, Chicago, IL, Sep. 2011.

[13] M. Budhia, G. A. Covic, and J. T. Boys, "Design and optimization of circular magnetic structures for lumped inductive power transfer systems," *IEEE Trans. Power Electron.*, vol. 26, no. 11, pp. 3096–3108, 2011.

[14] T. Imura, H. Okabe, T. Koyanagi, M. Kato, T. Beh, M. Ote, J. Shimamoto, M. Takamiya, and Y. Hori, "Proposal of wireless power transfer via magnetic resonant coupling in kHz-MHz-GHz," in *Proc. general conference 2010 IEICE (The Institute of Electronics, Information and Communication Engineers)*, Sendai, Japan, March 2010.

[15] "Improving the effectiveness, flexibility and availability of spectrum for short range devices," in *Document RAG07-1/17-E, , Radiocommunica-*
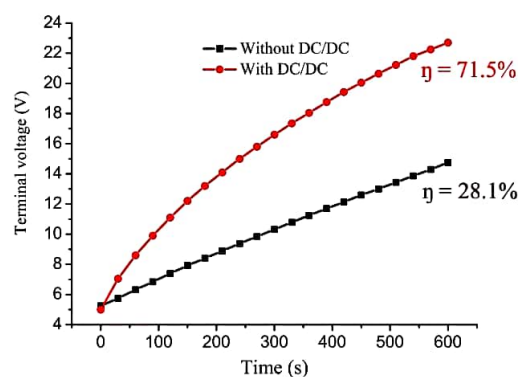
Fig. 15.   Ultracapacitors charging improvement using the cascaded boost-buck DC-DC converter.

tion Advisory Group, International Telecommunication Union, 2007.

[16] T. Imura, H. Okabe, and Y. Hori, "Basic experimental study on helical antennas of wireless power transfer for electric vehicles by using magnetic resonant couplings," in *Proc. The 5th IEEE Vehicle Power and Propulsion Conference (VPPC'09)*, Dearborn, MI, Sep. 2009, pp. 936–940.

[17] T. Imura and Y. Hori, "Maximizing air gap and efficiency of magnetic resonant coupling for wireless power transfer using equivalent circuit and neumann formula," *IEEE Trans. Ind. Electron.*, vol. 58, no. 10, pp. 4746–4752, 2011.

[18] D. M. Pozar, *Microwave engineering*.   John Wiley & Sons, 2009.

Xinen Zhu (S'04-M'09) received the B.Eng. (Hons.) degree in electronic and communication engineering from City University of Hong Kong, Hong Kong, in 2003, and the M.S. degree and the Ph.D. degree in electrical engineering from The University of Michigan at Ann Arbor, in 2005 and 2009 respectively.

He is currently an Assistant Professor with the University of Michigan-Shanghai Jiao Tong University Joint Institute, Shanghai Jiao Tong University, Shanghai, China. His research interests include wireless power transfer, tunable RF/microwave circuits, and ferroelectric thin films.

Dr. Zhu is a member of IEEE.

Minfan Fu received the B.S. and M.S. degrees both in electrical and computer engineering from University of Michigan-Shanghai Jiao Tong University Joint Institute, Shanghai Jiao Tong University, Shanghai, China in 2010 and 2013, respectively, where he is currently working toward Ph.D. degree.

His research interests include power electronics, control and the applications in wireless power transfer.

Chengbin Ma (M'05) received the B.S.E.E. degree from East China University of Science and Technology, Shanghai, China, in 1997, and the M.S. and Ph.D. degrees both in the electrical engineering from University of Tokyo, Tokyo, Japan, in 2001 and 2004, respectively.

He is a tenure-track assistant professor of electrical and computer engineering with the University of Michigan-Shanghai Jiao Tong University Joint Institute, Shanghai Jiao Tong University, Shanghai, China. Between 2006 and 2008, he held a post-doctoral position with the Department of Mechanical and Aeronautical Engineering, University of California Davis, California, USA. From 2004 to 2006, he was a R&D researcher with Servo Laboratory, Fanuc Limited, Yamanashi, Japan. His research interests include motion control and mechatronics, modeling and control of renewable and alternative energy systems such as electric vehicles, and wireless power transfer, etc.

Dr. Ma is a member of IEEE and ASME.